

# Phenomenological and Cosmological Implications of Neutrino Oscillations

**S. F. King**

Department of Physics and Astronomy,  
University of Southampton, Southampton SO17 1BJ, U.K.

**Abstract.** I discuss the implications of neutrino oscillations for neutrino mass patterns and mass matrices, and for neutrinoless double beta decay. I then go on to discuss the implications for cosmological relic density and dark matter, the galaxy structure limits on neutrino mass, nucleosynthesis, supernovae, cosmic rays and gamma ray bursts.

## 1. Introduction

Recent SNO results [1] when combined with other solar neutrino data especially that of Super-Kamiokande strongly favour the large mixing angle (LMA) MSW solar solution [2, 3] with three active light neutrino states, and  $\theta_{12} \approx \pi/6$ ,  $\Delta m_{21}^2 \approx 5 \times 10^{-5} \text{eV}^2$ . The atmospheric neutrino data [4] is consistent with maximal  $\nu_\mu - \nu_\tau$  neutrino mixing  $\theta_{23} \approx \pi/4$  with  $|\Delta m_{32}^2| \approx 2.5 \times 10^{-3} \text{eV}^2$  and the sign of  $\Delta m_{32}^2$  undetermined. The CHOOZ experiment limits  $\theta_{13} \lesssim 0.2$  over the favoured atmospheric range [5].

In this talk I shall briefly discuss some of the phenomenological and cosmological implications of these results.

## 2. Phenomenological Implications

### 2.1. Neutrino Masses and Mixing Angles

The minimal neutrino sector required to account for the atmospheric and solar neutrino oscillation data consists of three light physical neutrinos with left-handed flavour eigenstates,  $\nu_e$ ,  $\nu_\mu$ , and  $\nu_\tau$ , defined to be those states that share the same electroweak doublet as the left-handed charged lepton mass eigenstates. Within the framework of three-neutrino oscillations, the neutrino flavor eigenstates  $\nu_e$ ,  $\nu_\mu$ , and  $\nu_\tau$  are related to the neutrino mass eigenstates  $\nu_1$ ,  $\nu_2$ , and  $\nu_3$  with mass  $m_1$ ,  $m_2$ , and  $m_3$ , respectively, by a  $3 \times 3$  unitary matrix called the MNS matrix  $U_{MNS}$  [6, 7]

$$\begin{pmatrix} \nu_e \\ \nu_\mu \\ \nu_\tau \end{pmatrix} = \begin{pmatrix} U_{e1} & U_{e2} & U_{e3} \\ U_{\mu1} & U_{\mu2} & U_{\mu3} \\ U_{\tau1} & U_{\tau2} & U_{\tau3} \end{pmatrix} \begin{pmatrix} \nu_1 \\ \nu_2 \\ \nu_3 \end{pmatrix}. \quad (1)$$

Assuming the light neutrinos are Majorana,  $U_{MNS}$  can be parameterized in terms of three mixing angles  $\theta_{ij}$  and three complex phases  $\delta_{ij}$ . A unitary matrix has six phases but three of them are removed by the phase symmetry of the charged lepton Dirac masses. Since the neutrino masses are Majorana there is no additional phase

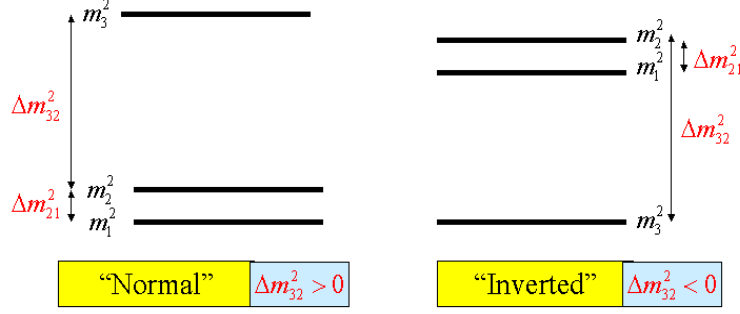


**Figure 1.** Alternative neutrino mass patterns that are consistent with neutrino oscillation explanations of the atmospheric and solar data.

symmetry associated with them, unlike the case of quark mixing where a further two phases may be removed.

There are basically two patterns of neutrino mass squared orderings consistent with the atmospheric and solar data as shown in Fig.1.

## 2.2. Neutrino Mass Matrices

In the flavour basis (in which the charged lepton mass matrix is diagonal), for a given assumed form of  $U_{MNS}$  and set of neutrino masses  $m_i$  one may “derive” the form of the neutrino mass matrix  $m_{LL}$ , and this results in the candidate mass matrices in Table 1 [8, 9]. In Table 1 the mass matrices are classified into two types:

Type I - small neutrinoless double beta decay

Type II - large neutrinoless double beta decay

They are also classified into the limiting cases consistent with the mass squared orderings in Fig.1:

A - Normal hierarchy  $m_1^2, m_2^2 \ll m_3^2$

B - Inverted hierarchy  $m_1^2 \approx m_2^2 \gg m_3^2$

C - Approximate degeneracy  $m_1^2 \approx m_2^2 \approx m_3^2$

Thus according to our classification there is only one neutrino mass matrix consistent with the normal neutrino mass hierarchy which we call Type IA, corresponding to the leading order neutrino masses of the form  $m_i = (0, 0, m)$ . For the inverted hierarchy there are two cases, Type IB corresponding to  $m_i = (m, -m, 0)$  or Type IIB corresponding to  $m_i = (m, m, 0)$ . For the approximate degeneracy cases there are three cases, Type IC corresponding to  $m_i = (m, -m, m)$  and two examples of Type IIC corresponding to either  $m_i = (m, m, m)$  or  $m_i = (m, m, -m)$ .

At present experiment allows any of the matrices in Table 1. In future it will be possible to uniquely specify the neutrino matrix in the following way:

1. Neutrinoless double beta effectively measures the 11 element of the mass matrix  $m_{LL}$  corresponding to

$$\beta\beta_{0\nu} \equiv \sum_i U_{ei}^2 m_i \quad (2)$$

**Table 1.** Leading order low energy neutrino Majorana mass matrices  $m_{LL}$  consistent with large atmospheric and solar mixing angles, classified according to the rate of neutrinoless double beta decay and the pattern of neutrino masses.

	Type I Small $\beta\beta_{0\nu}$	Type II Large $\beta\beta_{0\nu}$
<p>A</p> <p>Normal hierarchy</p> <p><math>m_1^2, m_2^2 \ll m_3^2</math></p>	<p><math>\beta\beta_{0\nu} \lesssim 0.0082 \text{ eV}</math></p> $\begin{pmatrix} 0 & 0 & 0 \\ 0 & 1 & 1 \\ 0 & 1 & 1 \end{pmatrix} \frac{m}{2}$	<p>–</p>
<p>B</p> <p>Inverted hierarchy</p> <p><math>m_1^2 \approx m_2^2 \gg m_3^2</math></p>	<p><math>\beta\beta_{0\nu} \lesssim 0.0082 \text{ eV}</math></p> $\begin{pmatrix} 0 & 1 & 1 \\ 1 & 0 & 0 \\ 1 & 0 & 0 \end{pmatrix} \frac{m}{\sqrt{2}}$	<p><math>\beta\beta_{0\nu} \gtrsim 0.0085 \text{ eV}</math></p> $\begin{pmatrix} 1 & 0 & 0 \\ 0 & \frac{1}{2} & \frac{1}{2} \\ 0 & \frac{1}{2} & \frac{1}{2} \end{pmatrix} m$
<p>C</p> <p>Approximate degeneracy</p> <p><math>m_1^2 \approx m_2^2 \approx m_3^2</math></p>	$\begin{pmatrix} 0 & \frac{1}{\sqrt{2}} & \frac{1}{\sqrt{2}} \\ \frac{1}{\sqrt{2}} & \frac{1}{2} & \frac{1}{2} \\ \frac{1}{\sqrt{2}} & \frac{1}{2} & \frac{1}{2} \end{pmatrix} m$	<p><math>\beta\beta_{0\nu} \gtrsim 0.035 \text{ eV}</math></p> <p>diag(1,1,1)m</p> $\begin{pmatrix} 1 & 0 & 0 \\ 0 & 0 & 1 \\ 0 & 1 & 0 \end{pmatrix} m$

and is clearly capable of resolving Type I from Type II cases according to the bounds given in Table 1 [10]. There has been a recent claim of a signal in neutrinoless double beta decay corresponding to  $\beta\beta_{0\nu} = 0.11 - 0.56 \text{ eV}$  at 95% C.L. [11]. However this claim has been criticised by two groups [12], [13] and in turn this criticism has been refuted [14]. Since the Heidelberg-Moscow experiment has almost reached its full sensitivity, we may have to wait for a next generation experiment such as GENIUS which is capable of pushing down the sensitivity to 0.01 eV to resolve this question.

2. A neutrino factory will measure the sign of  $\Delta m_{32}^2$  and resolve A from B.

3. Tritium beta decay experiments are sensitive to C since they measure the “electron neutrino mass” defined by

$$|m_{\nu_e}| \equiv \sum_i |U_{ei}|^2 |m_i| \leq 2.2 \text{ eV} (95\% \text{ C.L.}) \quad (3)$$

where the current laboratory limit is shown [15]. The prospects for improving on this bound are good: for example the KATRIN experiment has a proposed sensitivity of 0.35 eV.

Model building based on the different neutrino mass matrices in Table 1 was discussed separately at this meeting [16] and will not be considered further here.

### 3. Cosmological Implications

#### 3.1. Cosmological relic density and dark matter

In the early universe neutrinos were in thermal equilibrium with photons, electrons and positrons. When the universe cooled to temperatures of order 1 MeV the neutrinos decoupled, leading to a present day number density similar to photons. If neutrinos have mass they contribute to the mass density of the universe, leading to the constraint

$$\sum_i m_i \leq 28 \text{ eV} \quad (4)$$

corresponding to

$$\Omega_\nu h^2 \leq 0.3 \quad (5)$$

in the standard notation where  $\Omega_\nu$  is the ratio of the energy density in neutrinos to the critical energy density of the universe (corresponding to a flat universe), and  $h = H/100\text{km/Mpc/s}$  is the scaled Hubble parameter.

From the current tritium limit on the electron neutrino mass in Eq.3 together with the atmospheric and solar mass splittings we have a stronger constraint

$$0.05 \text{ eV} \leq \sum_i m_i \leq 6.6 \text{ eV} \quad (6)$$

corresponding to the range

$$0.0005 \leq \Omega_\nu h^2 \leq 0.07 \quad (7)$$

which implies that neutrinos cannot be regarded as the dominant component of dark matter, but make up between 0.1% and 14% of the mass-energy of the universe.

#### 3.2. Galaxy structure limits on neutrino mass

Recent results from the 2df galaxy redshift survey indicate that

$$\sum_i m_i < 1.8 \text{ eV (95\% C.L.)} \quad (8)$$

under certain mild assumptions [17]. This bound arises from the fact that the galaxy power spectrum is reduced on small distance scales (large wavenumber) as the amount of hot dark matter increases. Thus excessive amounts of free-streaming hot dark matter would lead to galaxies being less clumped than they appear to be on small distance scales.

However as discussed in [18] such bounds suffer from parameter degeneracies due to a restricted parameter space, and a more robust bound is

$$\sum_i m_i < 3 \text{ eV (95\% C.L.)} \quad (9)$$

Combined with the solar and atmospheric oscillation data this brackets the heaviest neutrino mass to be in the approximate range 0.04-1 eV. The fact that the mass of the heaviest neutrino is known to within an order of magnitude represents remarkable progress in neutrino physics over recent years. This implies that neutrinos make up less than about 7% of the total mass-energy of the universe, which is a stronger limit than that quoted in the previous sub-section.

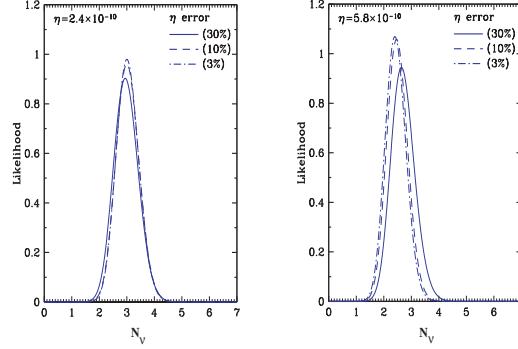


**Figure 2.** The distribution in the number of “neutrino species” (from [19]).

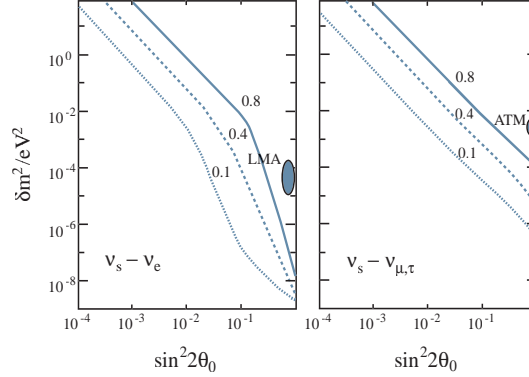


**Figure 3.** BBN constraints on active-sterile mixing parameters (from [19]).

### 3.3. Nucleosynthesis

The number of light “neutrino species”  $N_\nu$  (or any light species) affects the freeze-out temperature of weak processes which determine the neutron to proton ratio, and successful nucleosynthesis leads to the constraints on  $N_\nu$  as shown in Figure 2.

The limit on  $N_\nu$  applies also to sterile neutrinos, but they need to be produced during the time when nucleosynthesis was taking place, and the only way to produce them is via neutrino oscillations. This leads to strong limits on sterile-active neutrino mixing angles which tend to disfavour the LSND region, as shown in Figure 3. Note that these limits assume that the lepton asymmetry is not anomalously large [20].

### 3.4. Supernovae

It is well known that 99% of the energy of a supernova is emitted in the form of neutrinos, so one might hope that by studying supernovae one can learn something about neutrino physics. Indeed studies of the neutrino arrival times over a 10s interval from SN1987A in the Small Magellanic Cloud have led to the mass bound [21]

$$m_{\nu_e} \leq 6 - 20 \text{ eV} \quad (10)$$

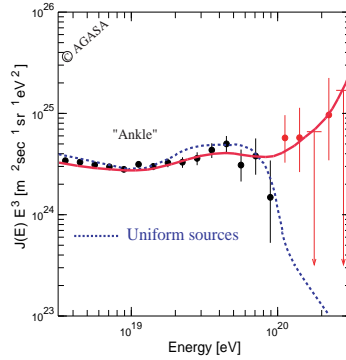


**Figure 4.** Scaled  $E^3$  spectrum of cosmic rays. The solid line is the prediction of the Z-burst model of [24] (from [19]).

The LMA MSW parameter range may also have some observable consequences for SN1987A [22, 23].

However it should be remarked that Supernova physics has difficulties simulating explosions, and understanding how the spinning neutron star remnant is kick-started.

### 3.5. Cosmic Rays

It has been a long standing puzzle why ultra high energy (UHE) cosmic rays are apparently observed beyond the Greisen-Zatsepin-Kuzmin (GZK) cutoff of  $5 \times 10^{19}$  GeV. The problem is that such cosmic rays appear to arrive isotropically, which would imply an extragalactic origin, whereas neither protons nor neutrons of such energies could have originated from more than 50 Mpc away due to their scattering off the cosmic background photons which would excite a delta resonance if the energy exceeds  $5 \times 10^{19}$  GeV. Yet despite this, several groups have reported handfuls of events above the GZK cut-off, for example the AGASA data shown in Figure 4. Also shown in this figure is the prediction of a Z-burst model which was invented to explain how the GZK cut-off could be overcome [24]. The basic idea of the Z-burst model is that UHE neutrinos can travel much further, and scatter off the relic background neutrinos to produce Z bosons within 50 Mpc. Neutrino mass is required to increase the Z production rate, so UHE cosmic rays and neutrino mass are linked in this model.

Recently data from Fly's Eye, Yakutsk and especially HiRes have brought into question whether the GZK cut-off is being exceeded at all. A recent analysis based on these data suggests that there might be no problem with the GZK cut-off [25]. On the other hand Fly's Eye and HiRes establish the cosmic ray energy from observing the fluorescence of Nitrogen molecules using a rather dated technique. The issue should be resolved soon by the Pierre Auger Observatory, which can both measure the shower's pattern on the Earth's surface, and the fluorescence of the shower in the air.

### 3.6. Gamma Ray Bursts (GRBs)

GRBs are distant ( $z \sim 1$ ), energetic and enigmatic. According to the fireball model (for a review see [27]) GRBs may result from the core collapse of a very massive supernova to a compact, rotating black hole. The energy is emitted in beamed relativistic fireball

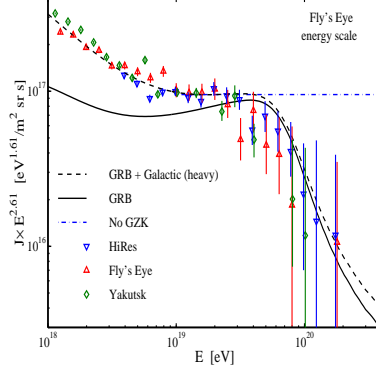


**Figure 5.** Recent data on cosmic rays (from [25]) which shows that the GZK cut-off might be respected after all.

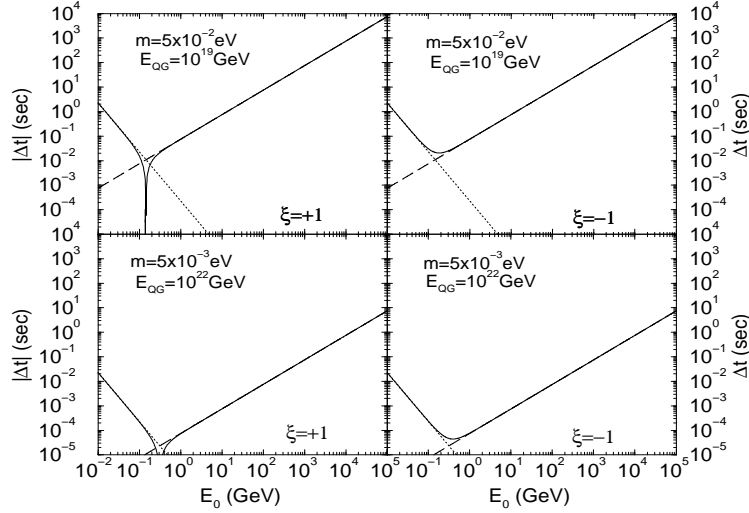


**Figure 6.** Time delays plotted against the neutrino energy. The downward sloping solid curve in each panel results from the effect of neutrino mass dominating at low energy, while the upward sloping solid curves are due to quantum gravity effects dominating at high energy (from [26]).

jets which are expected to contain copious neutrino fluxes. GRBs can thus be regarded as a high intensity, high energy neutrino beam with a cosmological baseline.

In some models of quantum gravity [28] neutrinos of mass  $m$  obey the dispersion relation

$$p^2 c^2 \approx E^2 \left(1 - \xi \frac{E}{E_{QG}}\right) - m^2 c^4 \quad (11)$$

where  $E_{QG}$  is the scale of quantum gravity. A consequence of this dispersion relation is that the effects of both quantum gravity and neutrino mass will cause time delays in the arrival times of neutrinos compared to low energy massless photons, as shown in Figure 6. Using the millisecond time structure of GRBs it may be possible to

measure neutrino masses from time of flight delays, in principle down to 0.001 eV [26]. However this estimate assumes complete understanding of GRBs, and large enough event rates, and in practice there are many theoretical and experimental challenges to be overcome.

#### 4. Conclusions

Future neutrino oscillation experiments, will give precious information about the mass squared splittings  $\Delta m_{ij}^2 \equiv m_i^2 - m_j^2$ , mixing angles, and CP violating phase. KATRIN and GENIUS will tell us about the absolute scale and nature of neutrino mass. We have seen that cosmology and astrophysics is also sensitive to the absolute values of neutrino masses. In the coming years there should be a fascinating interplay between neutrino physics on Earth and in the Heavens.

#### References

- [1] S. Biller, these proceedings.
- [2] S. Choubey, in these proceedings.
- [3] . Y. Smirnov, arXiv:hep-ph/0209131.
- [4] T. Kajita, these proceedings.
- [5] M. Apollonio *et al.* [CHOOZ Collaboration], Phys. Lett. B **466**, 415 (1999) [arXiv:hep-ex/9907037].
- [6] Z. Maki, M. Nakagawa and S. Sakata, Prog. Theor. Phys. **28** (1962) 870.
- [7] B. W. Lee, S. Pakvasa, R. E. Shrock and H. Sugawara, Phys. Rev. Lett. **38** (1977) 937 [Erratum-ibid. **38** (1977) 1230].
- [8] R. Barbieri, L. J. Hall, D. R. Smith, A. Strumia and N. Weiner, JHEP **9812** (1998) 017 [arXiv:hep-ph/9807235].
- [9] G. Altarelli and F. Feruglio, Phys. Rept. **320** (1999) 295.
- [10] S. Pascoli and S. T. Petcov, arXiv:hep-ph/0205022.
- [11] H. V. Klapdor-Kleingrothaus, A. Dietz, H. L. Harney and I. V. Krivosheina, Mod. Phys. Lett. A **16** (2001) 2409 [arXiv:hep-ph/0201231].
- [12] F. Feruglio, A. Strumia and F. Vissani, arXiv:hep-ph/0201291.
- [13] C. E. Aalseth *et al.*, arXiv:hep-ex/0202018.
- [14] H. V. Klapdor-Kleingrothaus, arXiv:hep-ph/0205228.
- [15] J. Bonn *et al.*, Nucl. Phys. Proc. Suppl. **110** (2002) 395.
- [16] G. Ross, these proceedings.
- [17] O. Elgaroy *et al.*, galaxy redshift survey,” arXiv:astro-ph/0204152.
- [18] S. Hannestad, arXiv:astro-ph/0208567.
- [19] K. Kainulainen and K. A. Olive, arXiv:hep-ph/0206163.
- [20] R. R. Volkas and Y. Y. Wong, Phys. Rev. D **62** (2000) 093024 [arXiv:hep-ph/0007185].
- [21] T. J. Loredo and D. Q. Lamb, Phys. Rev. D **65** (2002) 063002 [arXiv:astro-ph/0107260].
- [22] J.W.F. Valle, in these proceedings.
- [23] H. Minakata, H. Nunokawa, R. Tomas and J. W. Valle, Phys. Lett. B **542** (2002) 239 [arXiv:hep-ph/0112160].
- [24] G. Gelmini and G. Varieschi, arXiv:hep-ph/0201273.
- [25] J. N. Bahcall and E. Waxman, arXiv:hep-ph/0206217.
- [26] S. Choubey and S. F. King, arXiv:hep-ph/0207260.
- [27] G. Ghisellini, arXiv:astro-ph/0111584.
- [28] J. R. Ellis, N. E. Mavromatos, D. V. Nanopoulos and G. Volkov, Gen. Rel. Grav. **32** (2000) 1777 [arXiv:gr-qc/9911055].